5-GHz VLBI Imaging of the Gravitational Lens PKS 1830-211

Dayton L. Jones[1]
Jet Propulsion Laboratory, California Institute of Technology, Pasadena, CA, USA

Abstract

The strong radio source PKS 1830211 consists of two compact components located 011 opposite sides of a fainter ring of radio emission 1 arcsecond in diameter. 11 is the strongest radio source identified as a gravitational lens. Previous observations have shown that both compact components contain milliarcsecond-scale Structure. This paper presents 5 GHz VLBI images of both components made at two epochs separated by about 1 year. Significant changes in morphology are detected, which are not identical in the two components. This could result from different propagation delays along the paths from the background source to the two compact images we see. The usefulness of this source for cosmology is briefly discussed.

J Introduction

The 1 0-Jy radio source PKS 1830-211 was first suggested to be a gravitational lens by Rao and Subrahmanyan (1 988). More recent VLA and MERLIN observations have shown this source to be a beautiful example of a n Einstein ring gravitational lens (Jauncey *et al.* 1{}{} 1). The extragalactic nature of PKS1830 211, as inferred by Jauncey *et* (/1. (1991), has been confirmed by HI absorption measuren ients (Subrahmanyan, Kesteven, and te Lintel Hekkert 1992).

A pair of bright compact features is seen on opposite sides of the ring, and are believed to be two images of a portion of the background source. '1'11('s(! two compact components have been observed with VL B I in Australia at 0.84, 2.3 and 8.4 GHz, and by subsets of the VLBA at 1.6 and 22 GHz. In addition, two global (VLBA -| E VN) experiments were carried out in 1990 and 1991 al 5 GHz. This paper wilt concentrate on results from the 5 GHz observations. Preliminary results were presented in 1992 (Jones *et al.* 1{)93), but further analysis of the data has resulted in sig, nificantly higher dynamic range images since that time. Due to the higher quality images now available, it is seen that the morphology of both compact components has changed between the t wo 5 GHz epochs. The earlier images had shown obvious changes only in the NE component.

2 Observations and Data Analysis

The first 5 GHz VLBI epoch was 15 November 19{}(), and the second epoch was approximately 10 month s later 011 21 September 1991. Table 1 on the following page lists the antennas which observed during each epoch.

Rapid visibility beating due to the wide separation of tl ie two compact components in 1'1<S 1830-211 prevented fringe detection 011 trans-Atlantic and t rans-U. S. baselines.

[1] in collaboration with the Southern Hemisphere VLBI Experiment (SHEVE) team. Preston *et al.* (1993) lists the 34 current members of this collaboration.

Table 1: Antennas Participating in 5 GHz VLBI Experiments

Epoch	Antennas[a]
1990	s B W J2 No L K (: T] Pt La o
1991	s B W J2 No Kn Cb K G Kp Pt

Notes: [a] The antenna abbreviations are those of the U.S. and European VLBI network observing schedules.

Thus, the effective number of baselines was considerably less than implied by the number of antennas. The second epoch (1991) provided more data due to improved performance of several antennas, more short baselines, and an increase in the source flux density.

The Mk-II recording system was used, and all data were correlated at the JPL/Caltech Block II processor in Pasadena. Fringe fitting was performed with the AIPS task CALIB, and the resulting visibilities were transferred to the Caltech package **for** calibration, editing, and imaging. Errors were calculated from the scatter in the 2-second visibilities during coherent averaging of the data over 10 seconds. The visibility amplitudes were calibrated in the usual way based on measured system temperatures and (sometimes nominal) sensitivities of the antennas.

One complication caused by the widely-spaced, nearly equally strong double structure of this source is the need for an adequate source model for fringe fitting due to the frequent 180° jumps in phase on most baselines. Early attempts to use a default point source model were not very successful, but they did allow enough data to converge so that a crude initial map of the source could be made. The strongest few clean components from this map provided an adequate input model for fringe fitting to proceed successfully.

During imaging, only visibilities within $3 \times 10^7 \lambda$ of the aperture plane origin were used. Longer spacings suffered from low SNR, and the exclusion of these spacings also helped to make the (u, v) coverage more uniform between the two epochs. Imaging was carried out within the difference mapping program Difmap. Several iterations of phase self-calibration were followed by phase and amplitude self-calibration with decreasing solution smoothing times. In the early iterations, when the model accounted for less flux density than seen on the shorter baselines, the short baselines were excluded from the self-calibration solutions. This constraint was relaxed as the input model flux density approached that of the shortest baselines. Eventually the fit of the source model to the self-calibrated data achieved reduced χ^2 values less than unity for both epochs, suggesting that the visibility errors may be overestimated.

Image sizes of 1024 x 1024 pixels and 2048 x 2048 pixels were used for both epochs, with pixel sizes of 1.7 mas and 1.0 mas respectively. No significant differences resulted from the different map sizes. In all cases uniform weighting was applied during the Fourier inversions. Tight windowing was applied around the two compact components during deconvolution, until the final stage of mapping when the full map area was cleaned. Windowing within Difmap improved the initial speed of convergence between the image and self-calibrated data dramatically. An equally important feature of Difmap was its easy interactive data editing, which made this usually laborious task much faster and encouraged frequent examination

of the data after self-calibration iterations.

3 Results

Figure 1 below shows the full field of view mapped, illustrating the very large angular separation of the two compact components in this source.

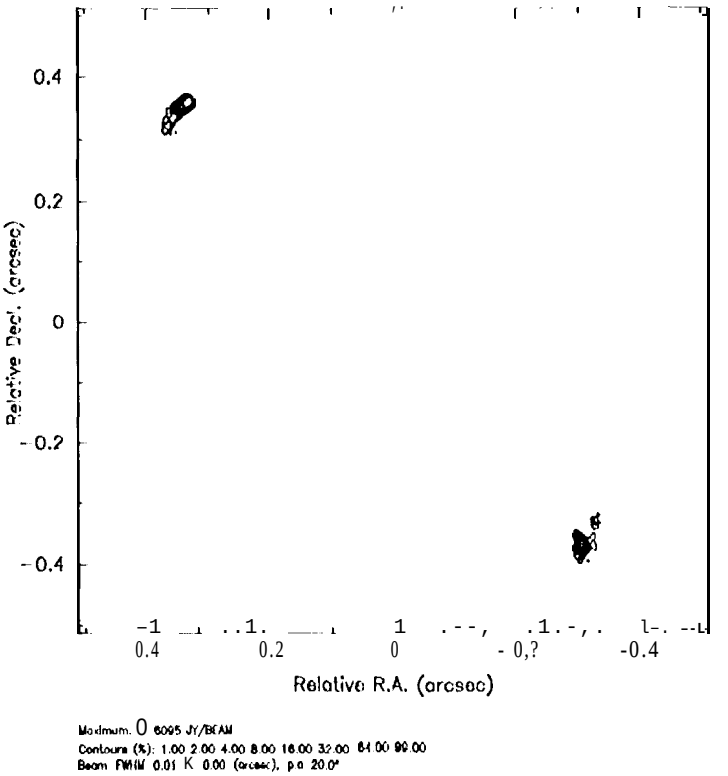

Figure 1 : Wide field (one arcsec square) map of 1'1{S 1830-21 1 at 5 GHz. The restoring beam FWHM is 9.8 X4.9 mas with the major axis along position angle 20.2 degrees. Contours are at -1, 1, 2, 4, 8, 16, 32, 64, and 99% of the peak (610 mJy/beam).

The main result of this work is shown in Figure 2 on the following page. This figure consists of closeup views of both compact components at both epochs. For ease of comparison, the second epoch images have been restored with the same clean beam as the first epoch, although the actual clean beam for the second epoch is considerably smaller than for the first epoch.

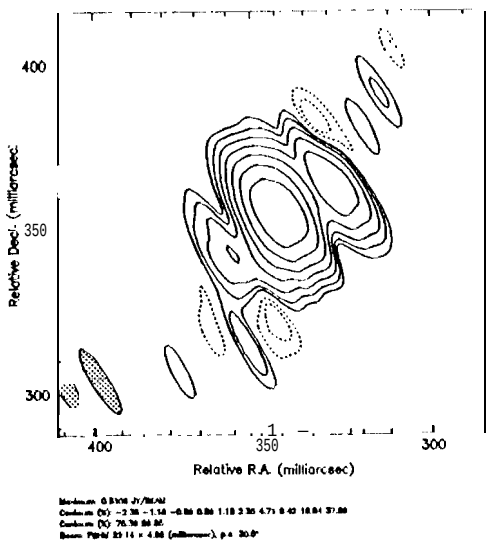

NE component in 1990

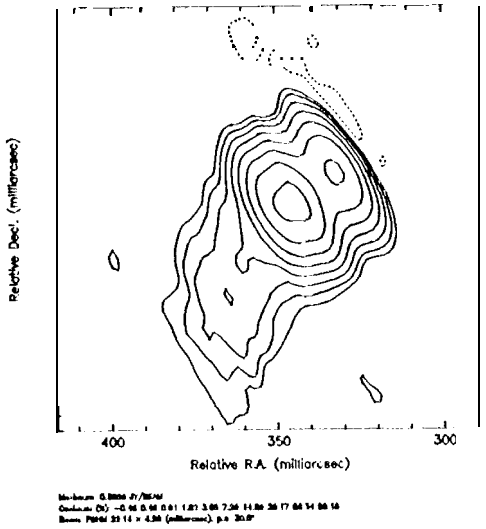

NE component in 1991

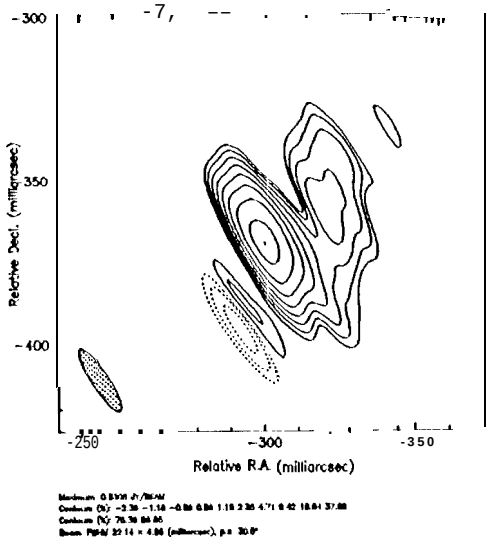

Sw component in 1990

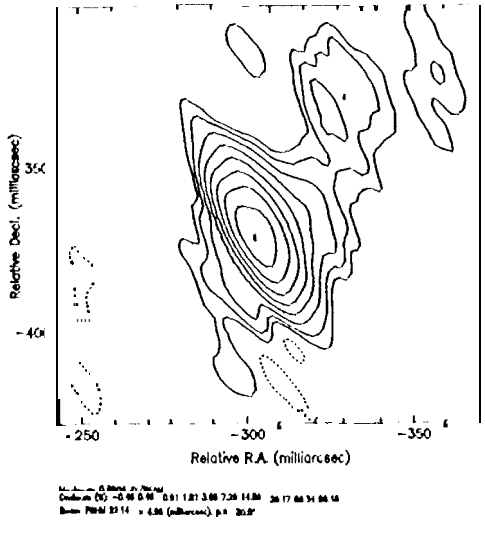

SW component in 1991

In all four of the images shown in figure 2, the same surface brightness contours have been used (-12.5, -6.25, -3.125, 3.125, 6.25, 12.5, 25, 50, 100, 200, 400 mJy/beam). In addition, a contour at 99% of the peak brightness was added to each figure (531 mJy/beam

for the 1990 epoch) (11 and 686 mJy/beam for the 1991 epoch). The restoring beam FWHM was 22.1×5.0 mas with the major axis along position angle 30.5 degrees.

Note that the peak brightness is 155 mJy/beam higher in the second epoch. This is consistent with the small increase in 5 GHz total flux density expected from an interpolation of 2.3 and 8.4 GHz total flux density changes (see Jauncey *et al.* 1993). The NE component appears to be responsible for most (if not all) of this brightening.

Examination of the images in figure 2 reveals substantial changes in both the NE and SW compact components. The NE component shows a much longer and stronger extension to the SE in 1991 than in 1990, and the SW component shows a large increase in separation between the brightest peak and the secondary feature to the NW. (This secondary feature is too weak to be seen in the maps shown by Jones *et al.* 1993.) For both the NE and SW components the position angle from the brightest peak to the apparently moving feature increases (counterclockwise rotation) between 1990 and 1991.

The separation between the three brightest features in the NE component (two of them barely resolved) did not change by more than about 2 mas between the 1990 and 1991 epochs. The relatively weak feature 18 ± 2 mas SE of the brightest peak in 1990 does not appear in the 1991 map, but if the brightest peak in the jet-like feature extending towards the SE in the 1991 map is identified as the same "knot" then its apparent transverse motion is 23 ± 3 mas/year.

For the SW component, in 1990 we see a weak feature with a peak 21 ± 2 mas NW of the brightest peak. In 1991, there is a weak feature with a peak 48 ± 2 mas NW of the brightest peak. If these are the same feature, the apparent transverse motion is 33 ± 3 mas/year. The implied motion of the weak features in both the NE and SW components of PKS 1830-211 is extremely rapid. However, the observed motion seen through a lens may be much faster than the true proper motion taking place in the background radio source. Also, of course, it is not possible to determine any proper motion unambiguously with only two epochs.

4 Conclusions

The fact that the changes seen in the two compact components are not identical could be explained by a difference in the propagation delay along the two lines of sight. An alternative possibility is that interstellar scattering within our galaxy is responsible for some of the observed changes in morphology. A VLBA experiment at 22 GHz, where such effects should be negligible even at the low galactic latitude of PKS 1830-211, is awaiting correlation. This experiment will help determine if the angular size of the components scales with λ^2 as expected from scattering.

Despite continuing efforts to obtain an unambiguous optical identification and redshift for PKS 1830211 (*e.g.*, Djorgovsky *et al.* 1992; Jauncey *et al.* 1992), the crowded field and optical faintness of the object have made this task difficult. Without knowing the distances to the lensing galaxy or the background radio source, the detailed models developed to explain this source (*e.g.*, Subrahmanyan, Narasimha, Rao, and Swarup 1990; Kochanek 1991; Nair, Narasimha, and Rao 1993; Kochanek and Narayan 1992) cannot lead to an estimate of H_0. If optical redshifts can be obtained in the future, the potential exists for an accurate H_0 determination due to the strength of the source and the resulting large quantity

of observational data available over a range of frequencies, time scales, and angular scales which can be used to constrain models of the lens.

I thank S. Unwin for providing absentee correlation of these data, and T. Pearson and M. Shepherd for their excellent VLBI data analysis software. This research was carried out at the Jet Propulsion Laboratory, California Institute of Technology, under contract with the National Aeronautics and Space Administration.

References

Djorgovski, S., Meylan, G., Klemola, A., Thompson, D. J., Weir, W. N., Swarup, G., Rao, A. P., Subrahmanyan, R., and Smette, A. 1992, *Monthly Notices Roy. Astron. Soc.*, **257**, 240.

Jauncey, D. L., *et al.* 1991, *Nature*, **352**, 132.

Jauncey, D. L., *et al.* 1992, in *Gravitational Lenses*, ed. R. Kayser, T. Schramm, and L. Nieser (Berlin: Springer Verlag), p. 333.

Jones, D. L., *et al.* 1993, in *Sub-arcsecond Radio Astronomy*, ed. R. J. Davis and R. S. Booth (Cambridge: Cambridge University Press), p. 150.

Kochanek, C. S. 1991, *Astrophys. J.*, **373**, 354.

Kochanek, C. S., and Narayan, R. 1992, *Astrophys. J.*, **401**, 461.

Nair, S., Narasimha, D., and Rao, A. P. 1993, *Astrophys. J.*, **407**, 46.

Preston, R. A., *et al.* 1993, in *Sub-Arcsecond Radio Astronomy*, ed. R. J. Davis and R. S. Booth (Cambridge: Cambridge University Press), p. 428.

Rao, A. P., and Subrahmanyan, R. 1988, *Monthly Notices Roy. Astron. Soc.*, **231**, 229.

Subrahmanyan, R., Narasimha, D., Rao, A. P., and Swarup, G. 1990, *Monthly Notices Roy. Astron. Soc.*, **246**, 263.

Subrahmanyan, R., Kesteven, M. J., and te Lintel Kekkert, P. 1992, *Monthly Notices Roy. Astron. Soc.*, **259**, 63.